Angled-Collimator SPECT (A-SPECT): An Improved Approach to Cranial Single Photon Emission Tomography

Peter D. Esser, Philip O. Alderson, Robin J. Mitnick, and Jeffrey J. Arliss

College of Physicians & Surgeons, Columbia University, New York, New York

A special 30° slant-hole collimator has been developed for rotating camera single photon emission computerized tomography (SPECT) that allows the camera to remain close to the patient's head throughout a standard 360° circular rotation. Compared with SPECT using parallel-hole collimation, angled-collimator SPECT (A-SPECT) yielded approximately a 30% increase in resolution without significant losses in sensitivity. The full width at half maximum in reconstructed transaxial images of Tc-99m line sources was 1.2 cm for the A-SPECT system compared with 1.6 cm for conventional SPECT, and A-SPECT yielded substantial improvements in modulation transfer function for the line source. A-SPECT images of phantoms and of patients with paranasal sinus disease were consistently superior in resolution to those of conventional SPECT. The findings suggest that A-SPECT will improve the quality of cranial images obtained with rotating camera SPECT systems.

Single photon emission computerized tomography (SPECT) has been used for several types of cranial imaging, including detection of abnormalities in the temporomandibular (TM) joints (*1*), facial bones (*2*), and paranasal sinuses (*3*), and for brain imaging with iodinated amines (*4–7*). Unfortunately, resolution and contrast in slices generated from rotating-camera SPECT images of the head are compromised by the large collimator-to-patient distances necessary with current commercial systems. This occurs because the camera head moves around the patient in a circular orbit with a radius that must be larger than that of the largest transverse section of the patient encountered by the orbit. In cranial imaging, a serious constraint is created by the shoulders. Since the orbit is circular, the shoulder-to-shoulder width necessitates a large orbiting radius that demands a gap between the camera and the head during the whole revolution. Attempts to increase resolution have used noncircular orbits (*8–11*) to reduce the distance between the moving detector and the head, or fan-beam collimation (*12,13*). We have pursued a different approach in search of improved resolution in cranial SPECT. We postulated that if the camera head of the tomographic unit were tilted at a fixed angle to the axis of rotation, it would be possible to move the camera head close to the cranium, still clearing the shoulders, and providing a full field of view. Orthogonal parallel-hole collimators would be unsuitable for this arrangement, so a slant-hole design (*14–18*) was used to develop an angulated collimator specifically suited for rotating camera SPECT. This paper describes this angulated collimator system and the results obtained during its application to phantoms and cranial studies in patients.

Received Nov. 2, 1983; revision accepted Jan. 10, 1984.

For reprints contact: Peter D. Esser, PhD, Div. of Nucl. Med., 622 West 168 St., New York, NY 10032.

METHODS

The angulated collimation approach to SPECT (A-SPECT) allows the collimator to move in a cone shaped path about the patient's head (Figs. 1 and 2). As the gantry arms move in a circle, the camera maintains the same angle with respect to the axis of rotation. Thus, at 90° and 270°, the camera will be opposite each shoulder at the edge of the patient's pallet and still be in close apposition to the cranium. Even though the camera is tilted, the collimator holes remain perpendicular to the axis of rotation. The slant angle of the collimator's holes is the same as the angulation of the camera head with respect to the axis of rotation. When the angle of slant is optimized, it permits the collimator to be tangent to both the lateral portion of the skull and the outer edge of the shoulders.

To optimize the slant of the collimator for patient studies, we investigated the tangential angle between the vertex of the head and shoulders of 48 consecutive subjects (24 M, 24 F) who were referred for conventional cranial scintigrams. The angle between the body axis and the head-shoulder tangent was measured bilaterally with the subjects standing. The average angle was 26 ± 2° (s.d.) so two collimators were designed* with hexagonal collimator holes at a 30° slant to the collimator's surface. The slant-hole collimators used in planar imaging typically are allowed ±5° of angular deviation across the face of the collimator. Our collimators were designed with tighter tolerances, to enhance their utility for

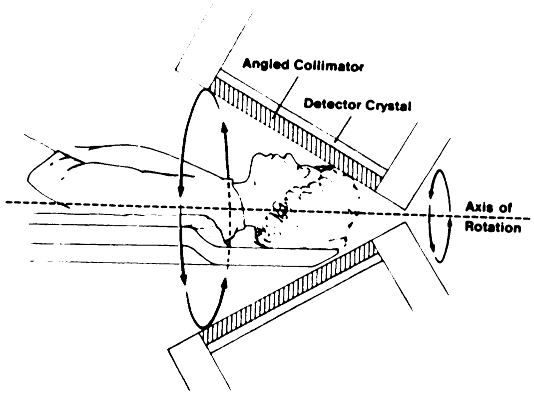

FIG. 1. Theoretical basis for use of tilted camera head and angled collimator is illustrated.

A-SPECT. The prototype collimator had 0.070-in. holes and was angled at 30° ± 3° to the collimator's face. The second collimator had 0.055-in. holes and an improved angular tolerance of ±1°. Both collimators were 1.0 in. in length, but differed in the way they were attached to the camera head. The prototype collimator was permanently mounted in a lead ring that had to be fastened to the camera with screws. The second version was a removable insert for a lead collar attached to the camera. Both collimator cores were precisely aligned in their mounting assemblies so that all holes would be vertical when the detector is at "12 o'clock". Two parallel-hole, nonangulated collimators with the same specifications—i.e., the same number, diameter and length of holes—were used to obtain conventional SPECT images for comparison with A-SPECT.

The gantry and detector system used for this study was a commercial model.† The camera head contained 61 photomultipliers and had a 15-in. field of view. The detector base was surrounded by a ring of 3 in. of lead to provide shielding for 511 keV. The detector's orbit was under motor control, with a digital readout in degrees displayed on the pendant gantry controller. Before each study, the camera head was tilted to zero degrees and checked with a level. The camera head was then tilted to the correct angulated position and maintained there by two cables attached with hand-tightened turn-buckles to a steel bar running between the gantry arms.

Digital data were acquired with standard commercial computer software‡. The unique features of the programmability of the gantry motion have been reported previously (*19*). All projections were acquired as 64 × 64 word-mode images. Most clinical acquisitions contained 90 projections with 20-sec acquisition time per image. Reconstructions also were generated with standard software. Daily flood fields were acquired with a thick water phantom (*20*) resting on the collimator, and periodic center-of-rotation checks were performed. With this system we found the camera's energy and uniformity corrections adequate to prevent artifacts in clinical images.

Comparisons of A-SPECT and conventional SPECT were performed on line sources and phantoms, as well as in patients referred for emission tomography of the paranasal sinuses. For patient studies we used values for standard man to determine that the average minimum radius of revolution for a cranial A-SPECT study should be about 13.2 cm at the center of the collimator (11.2 cm average radius for the adult cranium plus 2 cm for the pallet), compared with 25 cm (average orbiting radius to clear the shoulders) for conventional SPECT. We chose the expected center of the head as the distance for our phantom measurements because of our interest in evaluating paranasal sinus disease. A line source (plastic tube, 1.5 mm o.d., 0.5 mm i.d.) was extended from the head of the patient's pallet, parallel to its surface. The tube was supported in air by a thin aluminum sheath and was attached to the patient's pallet for additional support. The camera-collimator system then rotated around the line source with an orbital radius of 13.4 cm for A-SPECT and 25 cm for SPECT. During these revolutions the collimator face was tilted 30° to the axis of rotation for A-SPECT and was parallel to the axis for SPECT. The sensitivity of the angled collimators relative to those with parallel holes was investigated by replicate counting (6 trials each) of the activity from a 1.6 mCi Tc-99m source (160 cm^2 area) placed on each collimator over the same area of the detector.

Comparative studies also were performed on two phantoms§. The first was a radioactive ring with an external diameter of 5 in. and a thickness of 0.5 in. Inside the ring was nonradioactive water. Pairs of nonradioactive disks, 5 to 20 mm in diameter, were present in one side of the ring and similar sized doughnut-shaped objects with a radioactive center were present on the opposite side. The second phantom was 8.5 in. in diameter and consisted of nine pairs of radioactive foci in a plexiglas background. The pairs were separated by increasingly smaller distances (18 mm to 3 mm) moving from left to right. To compare the collimators, these phantoms were filled with activity and 100,000 counts were collected in each of 90 profiles. One pixel wide transaxial slices then were constructed from each set of data using a high-resolution Hanning filter (*21*). The total set of 130 reconstructed image slices was then presented to three observers who did not know which collimator produced each set of images. They were asked to choose the smallest observable defect in each set of images.

In addition to these phantom evaluations, 40 patients suspected of having inflammatory disease of the paranasal sinuses had A-SPECT tomograms, and three had SPECT head tomograms with both the angulated collimator system and a parallel collimator with the same resolution and sensitivity characteristics. Each comparison study was performed at the same session after a single injection of bone-seeking agent. Transaxial SPECT images from patients studied with both collimators were reviewed by a physician who had no knowledge of which collimator was used. He was asked to select the images with the best resolution and clarity.

Each patient was positioned to minimize the air gap between the collimator and the forehead. For most patients, the gantry arms were positioned at 20.5° to the axis of revolution, with the camera head at a 30° angle. Corrections for patient-to-patient anatomical differences were made by raising or lowering the patient's pallet, by changing the gantry arm angle, and by small shifts in the linear position of the gantry. The patient's head was secured to the table by Velcro straps (Fig. 2). To check clearance, the gantry always

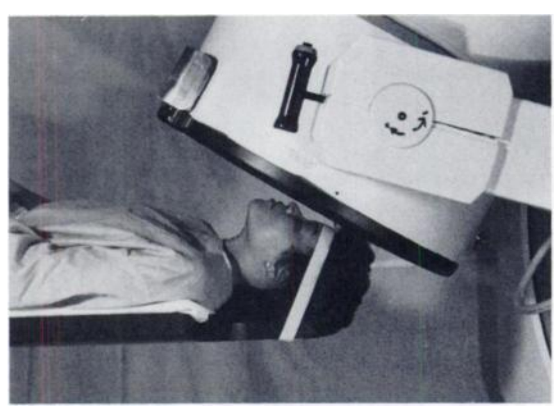

FIG. 2. Patient position for A-SPECT head tomogram. Gantry is shown at 0°. Camera head is tilted 30° and remains fixed at this angle while gantry revolves between 0 and 360°. Note close apposition of collimator to patient's head.

TABLE 1. COLLIMATOR PERFORMANCE

Hole angle	Hole size* (in.)	Measured relative sensitivity	FWHM† (mm)	FWTM† (mm)
0°	0.055	1.0	16.4	29.0
30	0.055	1.1	12.1	21.9
0	0.070	1.8	19.7	35.2
30	0.070	1.9	13.4	24.3

* Hexagonal holes, septa 0.010 in., bore length 1.0 in.
† At center of rotation for typical clinical radius of rotation (parallel hole: 25 cm, slant hole: 13.4 cm). Image matrix size was 64 X 64. Images acquired at 4° intervals.

was rotated manually through a complete circle before computer control was initiated. All motions other than gantry motion were locked out during automatic rotation, and a staff member remained with the patient to observe the procedure.

RESULTS

The specifications of the slanted collimators and the matching parallel-hole collimators are listed in Table 1, with the full width at half maximum (FWHM) and the full width at tenth maximum (FWTM) for their line spread functions. The modulation transfer functions in air obtained from these same experiments are shown in Fig. 3. As demonstrated in Table 1 and Fig. 3, the decrease in radius of revolution made possible by angulating the camera head produced 26% (0.055-in. slanted collimator) and 32% (0.070-in. slanted collimator) improvements in the FWHM, and significant improvements in MTF, without loss in sensitivity.

A transaxial slice through the 14-mm defects in the ring phantom is shown in Fig. 4 (left). The images were acquired with the high-resolution (0.055-in. holes) collimators. The defects are at 11 and 5 o'clock on the phantom ring. Each of three independent observers detected smaller defects (7mm diam) in the A-SPECT images than in images derived from conventional SPECT, where one observer correctly detected a 10-mm defect but the others only 14-mm defects. Four pixel wide slices from the second phantom are shown in Fig. 4 (right). Of the nine progressively smaller spaces between pairs of hot disks, four (ranging from 18mm to 9.2mm) can be seen clearly in the image generated from the slanted high-resolution collimator, whereas even the largest defect (18mm) is blurred in the image reconstructed from parallel-hole collimator data. In each case the A-SPECT images showed better resolution and more contrast than the corresponding SPECT images acquired with parallel-hole collimators.

A-SPECT images also showed better clarity and structural detail than SPECT images in each of the three patients who had both studies, and showed consistently good anatomic details of the facial skeleton in all other patients (Fig. 5). Clinical A-SPECT studies were well tolerated by the patients.

DISCUSSION

The results of the study support the theoretical advantages of using an angulated collimator for cranial SPECT. The close apposition of the camera to the patient's head throughout the revolution increases resolution by reducing the air gap necessary with parallel-hole collimation. The maximum distance from center of angulated collimator to axis of revolution is reduced from 25.0 to 13.4 cm, and this distance remains constant throughout the entire revolution. Thus, existing software can be used for all reconstructions. Actual improvements in resolution of ~30% were associated with this approach, as demonstrated by measurements on line sources and phantoms.

Note that with A-SPECT the holes along the craniocaudal diameter of the collimator will orbit with different radii. Resolution depends strongly on this radius, which in turn depends on the craniocaudal level of the plane of interest. Thus the most caudal portions of the angled collimator will have a radius of revolution as large as that in conventional SPECT, and will have a resolution comparable with that of SPECT. Fortunately, the structures viewed by this portion of the collimator are caudal to the face and are not in the field of interest (Figs. 1, 2, 6). Conversely, the holes viewing the top of the head will have a small orbiting radius and even better resolution than that listed for the center of the head region in Table 1. This should make this system well suited to brain imaging, since the brain will be beneath the most effective part of the collimator.

A-SPECT produces slight elongation of the image along the axis of rotation. As the camera head is tilted, the image of the patient's head is projected onto an increasingly larger area of the detector. Thus, a larger crystal surface is exposed to photons from the patient. Since the detector head is tilted on an axis perpendicular to the axis of revolution, the elongation occurs only along this axis. At a 30° angle, the elongation parallel to the axis of rotation is 1.15. This minor difference can be seen in sagittal and coronal sections (Fig. 6), but not in transaxial images. Corrections for this elongation can be made either in computer software or by changing the appropriate amplifier gains. However, the elongation has not been visually objectionable and has not impaired the interpretation of the tomographic images.

A-SPECT puts special stability requirements on the gantry of an orbiting camera, since gantry design has emphasized 0° detector angulation during rotation. Mispositioning of the camera head and collimator distortions can reduce the advantages of the angulated-collimator approach. On our prototype gantry, we used a bar across the arms to reduce detector wobble during rotation, but production versions of this gantry have been modified by the manufacturer to eliminate the need for the bar. In addition, collimators for A-SPECT must be manufactured to a precision not necessary for collimators used in planar imaging, i.e., A-SPECT collimators should be constructed precisely to a 30° slant and the angular deviation of the collimators must be kept as small as possible.

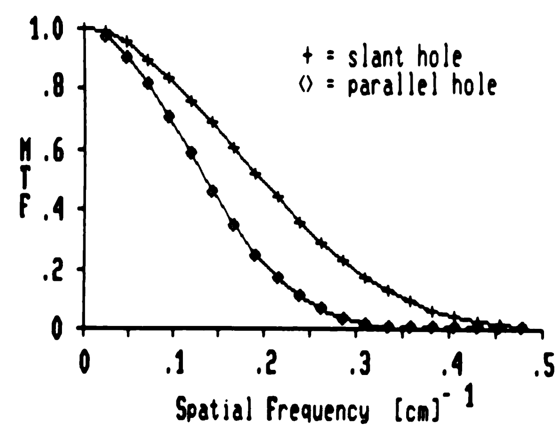

FIG. 3. Modulation transfer functions calculated from line spread functions of 0.055-in. collimators. Line sources were positioned on axis of rotation. Radii of rotation were 13.4 cm (slant) and 25 cm (parallel). Angled (slant-hole) collimator yielded substantially better performance.

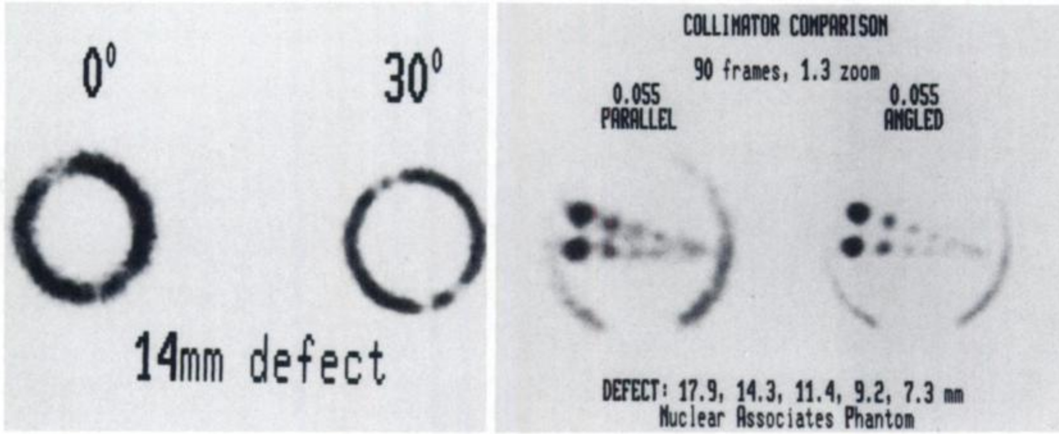

FIG. 4. Left: Reconstructed transaxial images through 14 mm defects in phantom with 0.5 in. thick Tc-99m activated outer ring and water-filled center (A). Parallel hole collimator (labeled 0° slant) images on left and 30° angled collimator on right. Axis of rotation was 11.8 cm from slant hole collimator. Note improved visibility of defects and increased sharpness in images obtained by angled collimator. Right: Reconstructed transaxial slices (B) of lucite phantom with foci of increased uptake and intervening defects. Axis of rotation was approximately 12.5 cm from slant collimator. Improved resolution and sharpness are seen in images obtained using the 30° angled collimator.

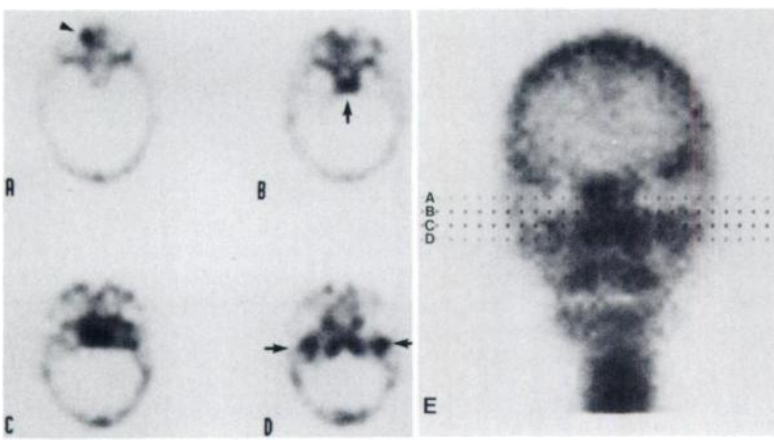

FIG. 5. A-E: Transaxial SPECt images (A–D) of patient with sinusitis. Slice A shows increased activity in right ethmoid region (arrow head) flanked by orbits. Slice B shows lower portion of orbits and increased activity in midline in sphenoid sinus (arrow). Slice C shows region of maxillary sinuses and inferior portion of sphenoid sinus, and D is at level of temporomandibular joints (arrows). Planar image E is provided for orientation to level of these slices.

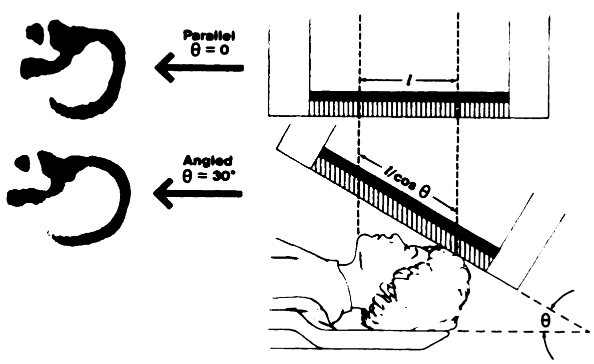

FIG. 6. Image elongation along axis of rotation is demonstrated. Distance, L, that image subtends on surface of detector increases as a function (L/cos θ) of camera head angulation. 30° tilt produces 1.15 elongation in sagittal plane.

Several studies have suggested other ways to increase the resolution of orbiting-camera tomographic systems. Both Croft et al. (*8,9*) and King et al. (*10*) described systems that executed noncircular orbits. However, to assure patient safety, the camera's distance from the axis of revolution was controlled by the operator during each change of position. Gottschalk et al. (*11*) showed that noncircular orbits implemented by a combination of rotational and translational motion of the detector could improve both resolution and uniformity. Their study was limited to imaging various phantoms and required modification of the back-projection algorithms. In an alternative approach to improve resolution, Coleman et al. reported a slight increase in resolution using a fan-beam collimator for imaging I-123-labeled compounds (*12*). However, fan-beam reconstruction requires special software not generally available.

The findings of our study suggest that the use of a special angulated collimator is a simple and safe means to increase substantially the resolution of cranial SPECT while preserving conventional circular orbits, a full view of the cranium, and the option to use conventional reconstruction software. The gains in resolution achieved by maintaining close apposition between the camera head and the patient throughout the orbit are not associated with losses of sensitivity. Our findings suggest that A-SPECT should provide an excellent method for cranial and brain emission tomography with orbiting-camera systems.

REFERENCES

1. O'Mara RE, Katzberg RW, Weber DA, et al: Skeletal imaging in temporomandibular joint (TMJ) disease. *J Nucl Med* 24:P42, 1983 (abst)

2. BROWN ML, KEYES JW, LEONARD PE, et al: Facial bone scanning by emission tomography. *J Nucl Med* 18:1184–1188, 1977
3. MITNICK RJ, POSTLEY JE, ESSER PD, et al: Comparison of single photon emission computed tomography (SPECT) in evaluation of patients with paranasal sinus disease. *J Nucl Med* 24:P58, 1983 (abst)
4. HILL TC, HOLMAN BL, LOVETT R, et al: Initial experience with SPECT (single photon computerized tomography) of the brain using n-isopropyl I-123-p-iodoamphetamine. *J Nucl Med* 23:191–195, 1982
5. KUHL DE, BARRIO JR, HUANG SC, et al: Quantifying local cerebral blood flow by n-isopropyl-P-[^{123}I]iodoamphetamine (IMP) tomography. *J Nucl Med* 23:196–203, 1982
6. ELL PJ, LUI D, CULLUM I, et al: Cerebral blood flow studies with I-123 labeled amines. *Lancet* (June 18):1348–1352, 1983
7. DRAYER B, JASZCZAK R, FRIEDMAN A, et al: in vivo quantitation of regional cerebral blood flow in glioma and cerebral infarction: validation of the HIPDM-SPECT method. *AJNR* 4:472-576, 1983
8. CROFT BY, TEATES CD, HONEYMAN JC: Single photon emission computed tomography of the liver. In *Digital Imaging*. Esser PD, ed. New York, Society of Nuclear Medicine, 1982, pp 271–282
9. CROFT BY, TEATES CD: Experience with single photon emission computed tomography of the liver. In *Emission Computed Tomography: Current Trends*. Esser PD, ed. New York, Society of Nuclear Medicine, 1983, pp 155–162
10. KING MA, SCHWINGER RB, ESSER PD, et al: Preliminary characterization of the properties of a new rotating SPECT imaging system. In *Emission Computed Tomography: Current Trends*, Esser PD, ed. New York, Society of Nuclear Medicine, 1983, pp 91–104
11. GOTTSCHALK SC, SALEM D, LIM CB, WAKER RH: SPECT resolution and uniformity improvements by noncircular orbits. *J Nucl Med* 24:822–828, 1983
12. COLEMAN RE, GREER KL, DREYER BP, et al: Collimation for I-123 imaging with SPECT. In *Emission Computed Tomography: Current Trends*. Esser PD, ed. New York, Society of Nuclear Medicine, 1983, pp 135–145
13. JASZCZAK RJ, CHANGE LT, MURPHY PH: Single photon emission computed tomography using multi-slice fan beam collimators. *IEEE Trans Nucl Sci* NS-26-610-618, 1979
14. FREEDMAN GS: Gamma camera tomography—Preliminary clinical experience. *J Nucl Med* 12:433, 1971
15. MUEHLLEHNER G: A tomographic scintillation camera. *Phys Med Biol* 16:87–96, 1971
16. CHANG W, LIN SL, HENKIN RE: A rotatable quadrant slant hole collimator for tomography (QSH): A stationary scintillation camera-based SPECT system. In *Single Photon Emission Computed Tomography*. New York, Society of Nuclear Medicine, 1980, pp 81–94
17. RATIB O, HENZE E, HOFFMAN E, et al: Performance of the rotating slant hole collimator for the detection of myocardial perfusion abnormalities. *J Nucl Med* 23:34–41, 1982
18. ROYAL H, PARKER JA, KOLODNY GM: Noncardiac, nontomographic applications of the slant-hole collimator: Concise communication. *J Nucl Med* 23:786–789, 1982
19. ESSER PD, MITNICK RJ, SELDIN DW, ALDERSON PO, KING MA, DOHERTY PW: Initial experience with an intelligent gantry system for single photon emission computed tomography. In *Emission Computed Tomography: Current Trends*. Esser PD, ed. New York, Society of Nuclear Medicine, 1983, pp 105–119
20. ESSER PD, ANGEL R, SELDIN DW, ALDERSON PO: An improved flood field phantom for single photon emission computed tomography (SPECT). *J Nucl Med* 24:P59, 1983 (abst)
21. LARSSON SA: Gamma camera emission tomography. *Acta Radiologica Suppl* 363, 1980

FOOTNOTES

* NuTech, New Haven, CT.

† Picker Dynascan® prototype.

‡ Medical Data Systems, Ann Arbor, MI.

§ Nuclear Associates/Victoreen, Carle Place, NY.